ACADEMIC PRESS

Available online at www.sciencedirect.com

SCIENCE DIRECT®

Journal of Magnetic Resonance 159 (2002) 175–182

JMR Journal of Magnetic Resonance

www.academicpress.com

High capacity production of >65% spin polarized xenon-129 for NMR spectroscopy and imaging

Anthony L. Zook, Bhavin B. Adhyaru, and Clifford R. Bowers*

Chemistry Department and National High Magnetic Field Laboratory, University of Florida, Gainesville, FL 32611-7200, USA

Received 24 May 2002; revised 8 October 2002

Abstract

A rubidium spin exchange optical pumping system for high capacity production of >65% spin polarized ^{129}Xe gas is described. This system is based on a fiber coupled multiple laser diode array capable of producing an unprecedented 210 W of circularly polarized light at the pumping cell with a laser line width of 1.6 nm. The ^{129}Xe nuclear spin polarization is measured as a function of flow rate, pumping cell pressure, and laser power for varying pumping gas compositions. A maximum ^{129}Xe nuclear polarization of 67% was achieved using a 0.6% Xe mixture at a Xe flow rate of 2.45 sccm. The ability to generate 12% polarized ^{129}Xe at rates in excess of 1 L-atm/h is also demonstrated. To achieve production of ^{129}Xe gas at even higher polarization will rely on further optimization of the pumping cell and laser beam geometries in order to mitigate problems associated with temperature gradients that are encountered at high laser power and Rb density.

1. Introduction

Spin exchange optical pumping of the spin-1/2 noble gases (i.e., ^{129}Xe and ^{3}He) is proving to be one of the most versatile methods for NMR signal enhancement [1,2]. The phenomenon can be conceptualized as a two step process: in the first step the hyperfine sublevels of an alkali metal vapor such as Rb are polarized by repeated absorption of polarized photons, while in the second step spin exchange collisions between the alkali and noble gas atoms leads to the accumulation of an enhanced nuclear polarization of the latter, sometimes referred to as *hyperpolarization*. While spin exchange optical pumping in low magnetic fields has been known since the 1960s [3,4], it was not until the demonstration by Raftery et al. [1] that the hyperpolarized noble gas can be separated from the alkali metal and employed as a pure gas in enhanced sensitivity high field NMR. Albert and co-workers [5] later demonstrated that hyperpolarized ^{129}Xe can be used to obtain in vivo magnetic resonance images. Hyperpolarized ^{3}He has been applied to imaging of lungs of humans [6], and now the technology of spin exchange optical pumping has even been commercialized [7] due to its excellent potential as a clinical diagnostic. The number of spectroscopic applications of hyperpolarized ^{129}Xe has also grown rapidly, and specific procedures and instrumentation for producing larger quantities of hyperpolarized noble gases have been recently developed [7,8]. Gains in the capacity of hyperpolarized ^{129}Xe that can be produced have been facilitated by the rapid development of solid-state laser diode array (LDA) systems in recent years.

Here we describe a hyperpolarized ^{129}Xe generator based on a 210 W laser diode array system, which is to our knowledge the highest optical power yet to be employed in Rb–^{129}Xe spin exchange optical pumping. The ability to perform spin exchange optical pumping experiments with this laser system affords a unique opportunity to study the optical power dependence of the ^{129}Xe nuclear polarization and to potentially identify unforeseen technical limitations that might be associated with performing optical pumping at very high laser power. In addition, the laser line width of 1.6 nm is relatively narrow compared to other multiple laser diode array laser systems at this power that have been described elsewhere.

* Corresponding author. Fax: 1-352-392-8758.
E-mail address: bowers@chem.ufl.edu (C.R. Bowers).

1090-7807/02/$ - see front matter © 2002 Elsevier Science (USA). All rights reserved.
PII: S1090-7807(02)00030-7

The rate of production of hyperpolarized ^{129}Xe by the spin exchange optical pumping is described by the following equation [8]:

$$\frac{d}{dt}2\langle K_z\rangle N_{\text{Xe-129}} = \eta I_{\text{abs}}. \quad (1)$$

Here, $\langle K_z\rangle$ is the average z-component of the ^{129}Xe nuclear spin, $N_{\text{Xe-129}} = [^{129}\text{Xe}]V_{\text{cell}}$ is the number of ^{129}Xe gas atoms polarized in a pumping cell volume V_{cell}, η characterizes the efficiency of Rb–Xe spin exchange transfer, and I_{abs} is the photon current absorbed by the Rb atom vapor. Eq. (1) indicates that higher capacity and/or higher polarization of ^{129}Xe can be achieved by increasing the optical absorption. Consequently, the ^{129}Xe polarization, $P_z = 2\langle K_z\rangle$, depends on the Rb vapor density, the pumping gas composition (Xe, N_2, and ^{4}He) and pressure, the pumping time and the spin relaxation rates in the vapor [8].

Prior to the advent of the LDA, the most common type of laser employed in Rb–Xe spin exchange optical pumping was the Ti:sapphire laser. Although the power is limited to a few watts, the line width of the Ti:sapphire is much narrower than the Doppler broadening of $\approx$1 GHz at ambient temperature. This is advantageous for spin exchange optical pumping at low pressures because the laser power is efficiently absorbed by the Rb vapor. The Ti:sapphire laser has proven to be well-suited to the production of small quantities (ca. 10 cm^3) of $>$50% polarized ^{129}Xe at pressures of $\approx$10 Torr [9]. With the advent of high power LDAs, much higher optical power is available, but laser line widths are typically 760–1500 GHz. For spin exchange optical pumping of ^{129}Xe, studies have shown that a ^{4}He/N_2/Xe mixture with a ^{129}Xe gas composition of a few percent provides the necessary pressure broadening for efficient optical absorption while minimizing spin destruction of the alkali metal atoms. The N_2 serves to quench the alkali-atom excited state, thereby reducing depolarization due to radiation trapping. With the greater optical power available with LDAs, much higher alkali metal atom densities can be pumped, and the rate of nuclear polarization of the ^{129}Xe gas is proportionally greater due to the increased rate of Xe–Rb spin exchange collisions. The higher rate of polarization makes it feasible to operate the polarizer in a continuous flow mode whereby a flowing stream of polarized Xe/N_2/He gas is generated. The hyperpolarized ^{129}Xe can be stripped cryogenically from the other pumping gas components. The LDA-based polarized gas generator is therefore desirable in applications requiring large quantities or an uninterrupted stream of polarized gas, including magnetic resonance imaging [10], enhanced NMR spectroscopy using hyperpolarized liquid ^{129}Xe [11–13], and phase cycled or two-dimensional NMR experiments [14].

As is evident from Eq. (1), two criteria which are relevant to the performance of a hyperpolarized gas generator are (i) the ^{129}Xe polarization achieved, P_z and (ii) the nuclear ^{129}Xe magnetization production rate, a quantity proportional to the product of the nuclear polarization and the ^{129}Xe flow rate at standard temperature and pressure. We refer to this product as the magnetization production factor (MPF). A survey of the recent spin exchange optical pumping literature [7–24] reveals a wide variation in the reported values of P_z and MPF. Some exceptional results include those of Appelt and co-workers [15], Fitzgerald et al. [11] and MITI [7] wherein values in the 18–21% range were reported, as well as Segebarth [24], Ruppert [18], and Chen et al. [19] who have reported data equivalent to MPF values in the 30–33 sccm% [25]. We note, however, that the collective results of this prior literature suggest that the ^{129}Xe polarization that can be achieved in LDA-based systems is substantially lower than that which can be obtained with a Ti:sapphire laser for relatively small quantities of ^{129}Xe. Ideally, a hyperpolarized ^{129}Xe generator would simultaneously achieve both high capacity and high polarization (e.g. 1 L/h with $P_z > 50\%$). Eq. (1) suggests that both higher polarization and high flow rates may potentially be obtained by increasing I_{abs} which can in principle be achieved by working at higher Rb density and higher laser power. To determine if this can be experimentally achieved requires an LDA system with higher power than has been available previously.

2. Experimental

The NHMFL [26] has supported the development of a polarized noble gas generator based on Rb–Xe spin exchange optical pumping. The gas handling system is similar to the one described by Driehuys et al. [8]. As shown in the schematic of Fig. 1, the cylindrical optical pumping cell is a 12.5 cm long borosilicate glass cylinder with 5.1 cm diameter optical flats sealed to each end. The internal volume is $V_{\text{cell}} = 250$ cm^3. The inlet and outlet ports consist of 6.4 mm OD borosilicate tubing fitted with Teflon stopcocks located a few cm from the points of attachment to the pumping cell. The transitions to 3.2 mm OD/1.6 mm ID PFA tubing are made using brass Swagelock reducing unions with Teflon ferrules. The inlet arm has a 1.5 cm long expanded region to accommodate a small quantity (approximately 0.3 g) of Rb metal. The cell is mounted such that its front window is tilted slightly away from the perpendicular orientation with respect to the incident laser beams. The cell is housed in an aluminum oven fitted with 20 cm diameter anti-reflection coated optical windows at the front and rear. The temperature in the oven is maintained by an Omega Engineering Model CN9000A controller that regulates the electrical current applied to a forced air resistive filament heater. A 43 cm diameter Helmholtz pair produces a 20 G field at the pumping cell.

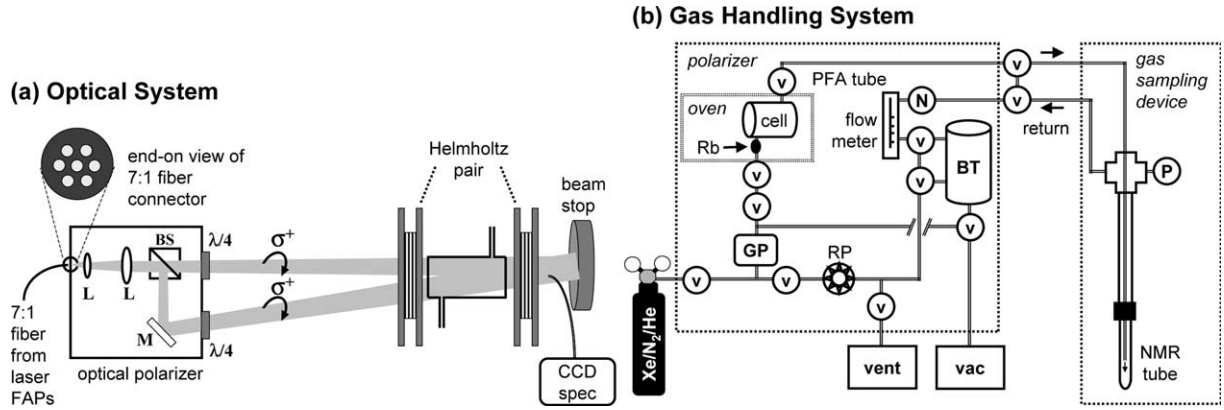

Fig. 1. Schematic of the NHMFL-UF Xenon-129 polarizer. (a) Optical polarizer and geometry of laser beams for excitation of the pumping cell. BS, beam splitting cube; L, lens; M, adjustable mirror; $\lambda/4$, quarter wave plate; OP cell, optical pumping cell; CCD spec, Ocean optics optical spectrometer. (b) Gas handling system. V, valve; P, pressure transducer; GP, gas purifier; RP, magnetically coupled recirculation pump; BT, ballast tank; vac, turbomolecular vacuum pump; N, needle valve; FAP, fiber array package laser diode arrays.

The gas handling system, shown in Fig. 1b, is designed to provide a continuous stream of the polarized ^{129}Xe gas mixture directly to the NMR probe or to a storage magnet for cryogenic separation and accumulation of hyperpolarized ^{129}Xe solid. The three different gas mixtures employed in this work were purchased from Spectra Gases (Branchburg, NJ) and used as received. Each consisted of equal mole percentages of Xe and N_2 at 1%, 2%, and 5%, with the balance made up of ^{4}He. The 1% mixture was enriched to 86% ^{129}Xe while the other mixtures contained natural Xe gas. The output of the storage cylinder is connected to a gas purifier (Model 35 K, Aeronex, San Diego, CA) to reduce the O_2, CO, CO_2, H_2, H_2O, and non-methane hydrocarbon content. The system pressure is monitored near the NMR probe and near the pumping cell using Baratron pressure transducers (Model 722A, MKS Instruments, Andover, MA). There is a 40 Torr pressure drop between the pumping cell and the NMR sampling device. The polarized ^{129}Xe gas mixture is delivered from the pumping cell to the NMR sampling device (see Fig. 1b) via a 4.7 m section of 1.6 mm ID PFA tubing. The flow rate is controlled on the return line by the needle valve on a variable area flowmeter (Model U-03217-06, Cole-Parmer, Vernon Hills, IL). After passing through the probe, the gas can either be vented to the atmosphere (in applications where the gas may have become contaminated) or recirculated back to the pumping cell. In the closed-cycle recirculation mode, flow is induced by a magnetically coupled gas recirculation pump (Model 51429, Thomas Ind., Sheboygan, WS). The entire gas handling system, including the glass pumping cell and sample tube, were pressure tested to approximately 10 atm.

The NHFML-UF polarized gas generator incorporates a laser system consisting of seven individual fiber array package (FAP) LDA units (Coherent Laser Corporation, Santa Clara, CA), each with an output of 30 W that can be independently tuned to 795 nm by thermoelectric temperature control. The combined optical profile has a line width of 1.6 nm (~760 GHz) at 210 W. The laser output and transmission through the optical pumping cell is continuously monitored with a fiber coupled optical spectrometer (model USB2000, Ocean Optics, Dunedin, FL). The fiber optic combiner assembly of the multiple FAP system, provided by Coherent, consists of seven individual anti-reflection coated fibers bonded into a hexagonal close-packed geometry using a special high-thermal conductivity epoxy. The output connector is clamped into a water-cooled copper block to reduce heating. The unpolarized beam emerging from the optical fiber assembly enters the optical polarizer (also provided by Coherent) where it is collimated before passing through a beam-splitting cube to divide the beam into horizontal and linear polarization components. The vertically polarized beam exits the optical polarizer through a quarter wave plate. The horizontally polarized beam is reflected by an adjustable mirror and exits through a second quarter wave plate with the fast axis aligned parallel to the slow axis of the first quarter wave plate. The mirror mount is adjusted such that the two beams intersect at the pumping cell 80 cm away. This optical polarizer arrangement permits the full power of the laser system to be circularly polarized even though the output of the fiber is unpolarized. The transmitted laser power (not absorbed by the Rb vapor) is captured by a water-cooled beam stop (Kentek Corporation, Pittsfield, NH).

As noted above, the rate of production of ^{129}Xe magnetization depends on the fraction of the laser power absorbed by the vapor. The absorbed photon current depends on the Rb vapor density which is determined by the cell temperature and its "conditioning." After extended use, the Rb metal gradually becomes contaminated with impurities such as oxygen and higher temperatures are required to obtain the optimal Rb

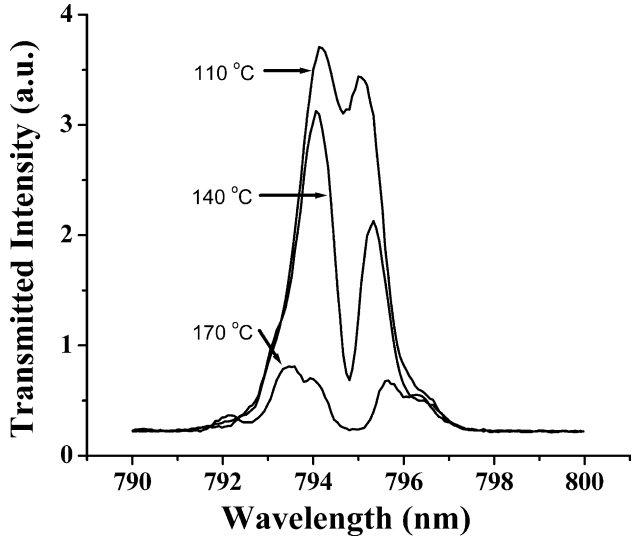

Fig. 2. Optical transmission spectra of the Rb vapor in the pumping cell at three different cell temperatures (100, 140, 170 °C) at a buffer gas pressure of 4.5 atm (1% Xe mixture) at 210 W laser power.

vapor density. Therefore, the temperatures reported in our study do not necessarily directly correlate to Rb atom density. Fig. 2 presents the optical transmission as a function of the pumping cell temperature at a gas pressure of 4.5 atm. At 110 °C, the Rb density is too low and the light is not absorbed, while at 170 °C the density is too high, and in this case the pumping light does not reach the back of the cell. At 140 °C the Rb will be optimally excited over the entire pumping cell volume.

3. Results and discussion

We now outline the procedure for calculating P_z and MPF from the experimental data. The ^{129}Xe nuclear polarization enhancement factor, $\mathscr{E}$, is the ratio of the enhanced polarization P_z to the thermal equilibrium (field polarized) polarization, P_z^{ref}. The enhancement factor at a specified field and temperature can be experimentally determined from the ratio of the NMR signal obtained in a single shot acquisition from one mole of laser polarized ^{129}Xe gas, $\tilde{S}$, and the reference signal obtained in single shot from one mole of thermally polarized gas, $\tilde{S}^{\mathrm{ref}}$. Thus, $\mathscr{E} = P_z/P_z^{\mathrm{ref}} = \tilde{S}/\tilde{S}^{\mathrm{ref}}$, which gives an expression to calculate the polarization of the hyperpolarized gas

$$P_z = P_z^{\mathrm{ref}} S_{\mathrm{m}}/S_{\mathrm{m}}^{\mathrm{ref}} = P_z^{\mathrm{ref}}\mathscr{E}. \quad (2)$$

In the high-temperature approximation, $P_z^{\mathrm{eq}} = \gamma\hbar H_0/2kT^{\mathrm{ref}} = 8.85\times10^{-6}$ at 300 K and $H_0 = 9.4T$. The raw FT NMR signal integrals S and S^{ref} of the hyperpolarized and thermally polarized reference samples need to be corrected for the number of moles of ^{129}Xe and the number of FIDs accumulated ($N_{\mathrm{s}}^{\mathrm{ref}}$ or N_{s}) in each experiment. For the thermally polarized reference sample, the correction factor is $\tilde{S}^{\mathrm{ref}} = S^{\mathrm{ref}}\ (n^{\mathrm{ref}}\cdot N_{\mathrm{s}}^{\mathrm{ref}})^{-1}$, where $n^{\mathrm{ref}} = (\pi r_{\mathrm{ref}}^2 l)p^{\mathrm{ref}}f^{\mathrm{ref}}/RT^{\mathrm{ref}}$ is the number of moles of ^{129}Xe gas contained in the cylindrical detection region of length l and radius r_{ref}, f^{ref} is the fractional isotopic abundance of ^{129}Xe in the thermal reference, and p^{ref} is the pressure of the thermal reference. Collecting all of these factors

$$\mathscr{E} = \frac{S}{S^{\mathrm{ref}}}\times\frac{N_{\mathrm{s}}^{\mathrm{ref}}}{N_{\mathrm{s}}}\times\frac{f^{\mathrm{ref}}}{f}\times\frac{p^{\mathrm{ref}}}{p}\times\frac{\chi_{\mathrm{Xe}}^{\mathrm{ref}}}{\chi_{\mathrm{Xe}}}\times\frac{T}{T^{\mathrm{ref}}}\times\left(\frac{r_{\mathrm{ref}}}{r}\right)^2. \quad (3)$$

The characteristics of the sealed thermal equilibrium reference sample and of the hyperpolarized sample are listed in Table 1. The thermal reference sample consists of a flame-sealed NMR tube containing 5 atm of xenon gas (natural isotopic composition) and 0.26 atm of oxygen to reduce the ^{129}Xe relaxation time to 1.9 s [27]. For improved signal to noise 64 FIDs were summed using an acquisition recycle delay of 30 s.

For instance, substituting the parameters for hyperpolarized sample #2 into Eq. (3) yields an enhancement factor $\mathscr{E} = 76,100$ and a polarization of $P_z = 67.3\%$. This calculation assumes that the laser polarized gas mixture has cooled to room temperature ($T = T^{\mathrm{ref}}$) during the transit through the 4.7 m × 1.6 mm ID PFA tubing to the NMR coil.

3.1. Dependence on flow rate

The ^{129}Xe polarization was measured as a function of flow rate through the pumping cell in continuous flow

Table 1
Experimental parameters used to calculate ^{129}Xe polarization

	Reference sample	Hyperpolarized sample #1	Hyperpolarized sample #2
Total pressure	5.26 atm	2.61 atm	2.44
Temperature	300 K	300 K	300 K
Xe mole fraction, χ_{Xe}	0.95	0.01	0.0059
^{129}Xe isotopic fraction, f	0.264	0.86	0.264
Sample tube ID, $2r$	7.9 mm	5.4 mm	5.4 mm
# FIDs accumulated, N_{s}	64	1	1
Signal integration, S	1.00	6.49	1.60
Enhancement factor, $\mathscr{E}$	–	52,200	76,100
^{129}Xe polarization, P_z	8.85×10^{-4}%	46.2%	67.3%

mode. The bulk flow rate F of the gas mixture determines the average residence time $\tau_{res} = V_{cell}/F$ of a ^{129}Xe atom in the pumping cell. Fig. 3 shows a plot of $\mathscr{E}$ as a function of the bulk pumping gas flow rate (in mL/min) at a pressure of 4.5 atm. A rapid increase in polarization is observed with increasing flow up to roughly 100 mL/min before leveling off. At flow rates >150 mL/min, $\mathscr{E}$ remained nearly constant up to 540 mL/min, the highest flow rate tested. Similar results (not shown) were obtained in the 2.7–4.5 atm range. At $F = 150$ mL/min, $\tau_{res} = 100$ s, while the transport time in the PFA tubing is about 3.6 s. Therefore, the residence time is long compared to the ^{129}Xe spin exchange optical pumping time of γ_{se}^{-1} which sets the time-scale for reaching the steady ^{129}Xe polarization according to $P_z(t) \approx P_{Rb}(1 - \exp(-\gamma_{se}t))$. A theoretical estimate of $\gamma_{se}^{-1} \approx 22$ s was reported for similar conditions of temperature and gas composition in [8]. Since a lower flow rate will only increase the residence time in the pumping cell, the sharp increase in polarization over the 35–100 mL/min range is most likely due to increased relaxation in the PFA tubing during transit through zero field.

3.2. Dependence on pumping gas pressure

We also studied the dependence of P_z on the gas pressure using two different pumping gas compositions. There are several previous reports indicating the necessity to use pressures in the 7–10 atm range in order to increase the optical absorption by pressure broadening of the Rb resonance line. As demonstrated in Fig. 4, the highest value of P_z is achieved at only 2.5–3 atm in the UF-NHMFL system in both the 1% and 2% Xe mixtures. This is most likely a consequence of the reduced laser line width of 1.6 nm of the LDA used in the present work. The ability to pump efficiently at reduced pressure is advantageous since Rb spin destruction is reduced [8].

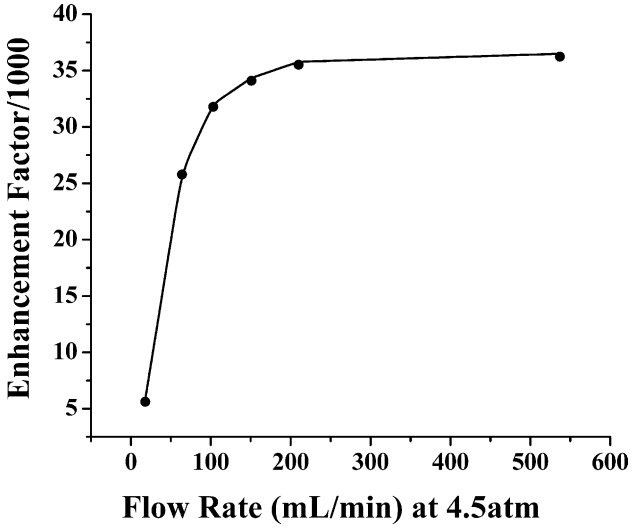

Fig. 3. NMR signal enhancement factor, $\mathscr{E}$ (defined in the text), as a function of the pumping gas flow rate at a system pressure of 4.5 atm (1% Xe mixture) and a pumping cell temperature of 150 °C and 210 W laser power. The enhancement factor is calculated from the laser polarized and reference signals using Eq. (3).

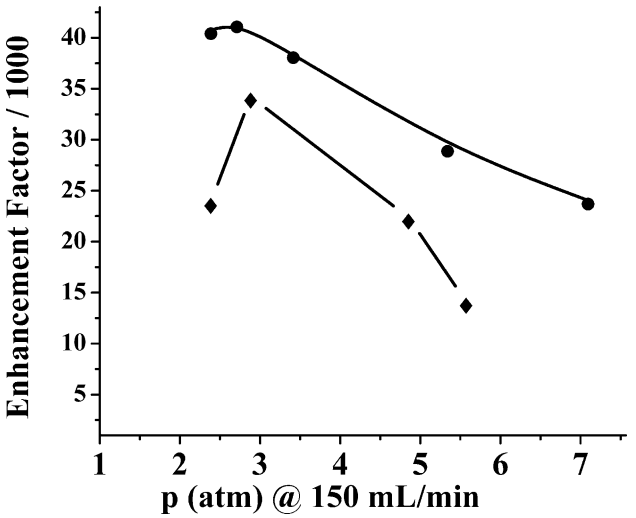

Fig. 4. NMR signal enhancement factor, $\mathscr{E}$ (defined in the text), as a function of the system pressure at a constant flow rate of 150 mL/min. Circles: 165 °C, 1% Xe mixture at 150 W. Diamonds: 130 °C, 2% Xe mixture at 210 W. The enhancement factor is calculated from the laser polarized and reference signals using Eq. (3).

3.3. Dependence on pumping gas composition

Typical performance characteristics of the UF-NHMFL hyperpolarized ^{129}Xe generator operating in the continuous flow mode with a variety of gas compositions and flow rates are presented in Table 2. The effect of percentage Xe composition in the pumping gas mixture was systematically studied in the 0.6–5% range using the experimental arrangement shown in Fig. 5. The polarizer and sampling loop (consisting of a glass cold-trap, pressure relief valve, NMR sample tube, a three-way valve to high vacuum, and a bypass loop) were filled with 2.6 atm of a 2% Xe, 2% N_2, 96% He gas mixture and allowed to mix throughout the polarizer and sample loop at a high flow rate. The pumping cell was heated to 145 °C Rb and irradiated with the laser set at 180 W. Xenon was removed from the gas mixture by immersing the cold-trap in a dewar of liquid N_2. After collecting solid Xe for a predetermined time interval, the sample loop was isolated from the polarizer using the three way valves. The gas remaining in the polarizer was recirculated through the pumping cell, ballast tank and bypass loop to ensure thorough mixing of the gas. To quantitatively determine the amount of Xe that was removed by the trap, the sample loop and trap were evacuated. Following evacuation, the sample loop and trap were isolated from the vacuum line, and the Xe that had been collected in the cold trap was allowed to warm up to a room temperature gas. The amount of Xe

Table 2
Typical UF-NHMFL polarizer data obtained in continuous flow production mode with various gas mixtures and flow rates

Laser power (W)	P_z (%)	Xe:N_2:He composition	^{129}Xe abundance	Xe flow rate (sccm)	MPF
>150	67.	0.60:2.0:97.4	0.264	2.45	43.
210	40.	1:1:98	0.86	4.8	160[a]
210	23.	2:2:96	0.264	7.44	45.
210	12.	5:5:90	0.264	18.6	59.

[a] Experiment with xenon gas enriched to 86% xenon-129.

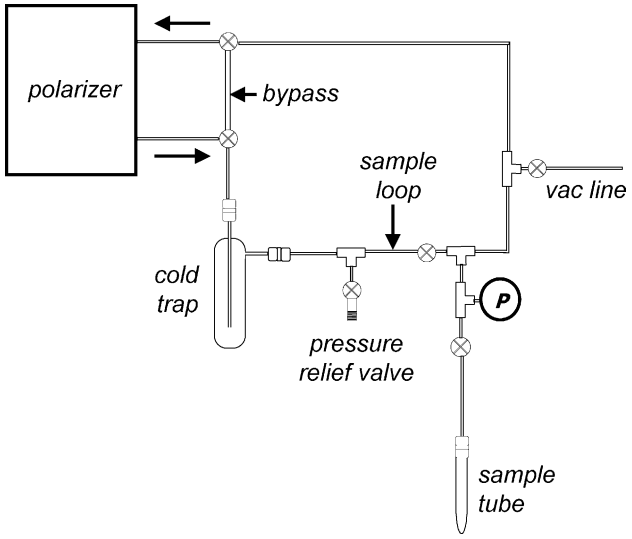

Fig. 5. Experimental apparatus used to vary the percentage Xe composition in the gas mixture.

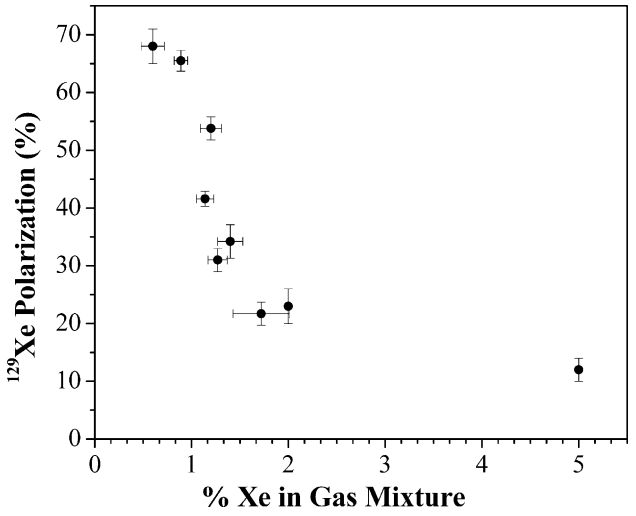

Fig. 6. Dependence of the ^{129}Xe polarization on the percentage Xe composition in the pumping gas mixture. The Xe fraction was varied and the experiment was performed using the apparatus shown in Fig. 5 and according to the procedure described in the text.

removed was determined from the pressure and the known volume of the trap/sample loop. After recording the pressure, the sample loop was evacuated once again. A sample of the gas in the polarizer loop was obtained by quickly opening the three-way valve to expand the gas into the sample tube for NMR detection by a single transient. It should be noted that this procedure minimizes wall relaxation in the delivery tubing which traverses regions at low magnetic field, and the ^{129}Xe polarization is not expected to be significantly reduced from the its value inside the pumping cell. To prepare for the next experiment at a different Xe fraction, the entire polarizer and sample loop was re-filled with the 2% Xe gas mixture and vented 3–4 times to ensure the mixture contained 2% Xe. The procedure was repeated with varying Xe collection time intervals to condense different amounts of Xe from the pumping gas mixture. The gas flow rate, laser power, and pumping cell temperature were kept constant throughout the experiments. The data that resulted from this procedure are shown in Fig. 6, illustrating that polarization values approaching 70% are obtained at 0.6% Xe. The highest ^{129}Xe polarization obtained in this mode was 67.% using the 0.6% Xe pumping gas mixture at a Xe flow rate of 2.45 sccm which is, to our knowledge, the highest level of ^{129}Xe polarization achieved in an LDA-based ^{129}Xe polarizer to date.

3.4. Dependence on laser power

The ability to perform spin exchange optical pumping experiments with a laser power up to 210 W affords the opportunity to study the optical power dependence of the ^{129}Xe nuclear polarization. For example, as shown in Fig. 7, at a pumping cell temperature of 140 °C and with a 1% Xe mixture (enriched to 86% ^{129}Xe) the ^{129}Xe nuclear polarization increases linearly with laser power up to 150 W and then levels off. When the laser power dependence is run at 145 °C with the 0.6% Xe mixture (natural abundance ^{129}Xe) a similar trend is observed but with the polarization reaching > 60% above 150 W excitation power. These curves are attributed to the saturation of the optical transition. In principle, the saturation could be avoided by increasing the temperature in order to increase the Rb density. However, temperatures above 145 °C proved to be problematic when exciting high Rb vapor density at laser powers in excess of 150 W. Under these conditions substantial heating of the gas occurred due to optical absorption and subsequent conversion into rotational and transla-

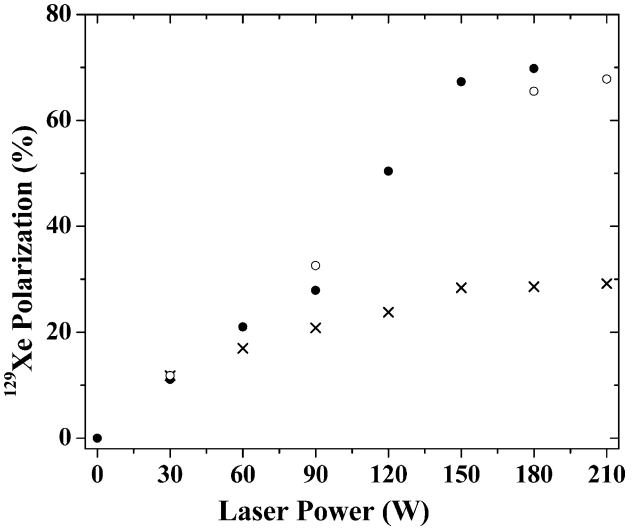

Fig. 7. NMR signal enhancement factor, $\mathscr{E}$ (defined in Eq. (3)), vs. laser power. The crosses correspond to optical pumping with a 1% Xe gas mixture at a pumping cell pressure of 2.6 atm, a temperature of 140 °C, and a flow rate of 150 mL/min. The data represented by the filled and open circles correspond to two different trials with a 0.6% Xe at 145 °C. A bulk flow rate of 170 mL/min at 2.44 atm was employed in these experimental runs.

tion excitation. Rotational heating of nitrogen in $Rb/Xe/N_2$ mixtures under high power optical pumping conditions has been studied by Raman scattering measurements [28]. Conversion to translational energy resulted in bulk gas temperatures 200 °C the wall temperatures. Using a thermocouple sensor we measured thermal gradients in excess of 20 °C across the 12.5 cm length dimension of the pumping cell. At elevated temperatures, the cell temperature became unstable because the heating produces an increased Rb density that in turn further increases the optical absorption. As the region near the front window becomes optically dense, the laser light does not effectively pump the Rb vapor near the rear of the cell. Thus, it was found to be necessary to constantly monitor the temperatures at the front and rear windows of the pumping cell with independent thermocouple sensors to avoid large temperature gradients. Heating, thermal gradients, and the resulting temperature control problems made it too difficult to obtain a complete laser power study at pumping cell temperatures 150 °C.

3.5. Spin transfer efficiency

Finally, we estimate the spin transfer efficiency achieved with our continuous flow spin exchange optical pumping system under the conditions that yielded the highest polarization. This can be compared to the value reported in the original measurements of Bhaskar et al. [29] who obtained $\eta = 0.043 \pm 0.006$ for the Rb–^{129}Xe system. The spin transfer efficiency is reportedly independent of both laser power and temperature [29]. The effective spin transfer efficiency in a continuous flow polarizer when $\tau_{res} \gg \gamma_{se}^{-1}$ is

$$\eta_{eff} = \frac{2\langle K_z \rangle f \cdot F \cdot \chi_{Xe}}{I_{abs}}, \tag{4}$$

where χ_{Xe} is the mole fraction of Xe in the pumping gas. From Fig. 2 it is estimated that at a laser power of 150 W, only 10–20% of the incident radiation is absorbed by the vapor. Accounting for additional reflection losses at the pumping cell and oven windows, the absorbed photon current at 795 nm is roughly $I_{abs} = 6.0 \times 10^{19}\,s^{-1}$. The highest polarization of $2\langle K_z \rangle = 0.67$ was achieved using a ^{129}Xe flow rate of 2.45 sccm at 0.6% Xe (corresponding to a bulk gas flow rate of 170 mL/min at 2.44 atm), yielding $\eta_{eff} \approx 3.2\times\ 10^{-3}$ using Eq. (4), implying that roughly $\eta_{eff}^{-1} \approx 310$ photons, on average, are involved in each ^{129}Xe spin flip. This is a substantially higher number than the 23 photons per spin flip reported in reference [29] for a sealed pumping cell experiment. The lower efficiency in our flow pumping cell arrangement can largely be accounted for by the average residence time of $\tau_{res} = V_{cell}/F = 87$ s which is a factor of about four greater than the spin exchange time of $\gamma_{se}^{-1} \approx 22$ s reported in [8] under similar experimental conditions. This implies that the same level of ^{129}Xe polarization could be sustained at Xe flow rates of at least 10 sccm. In principle, this would yield values within a factor of 3 relative to the $1/\eta = 23$ spin flips per photon absorbed as reported in [29]. The remaining discrepancy may be partially attributed to increased spin rotation losses resulting from the increased gas temperatures at high Rb densities and laser power absorption. Variable flow rate studies with $F > 600$ mL/min were not possible with the existing apparatus, but Fig. 3 does confirm that the polarization achieved in our polarized gas generator remains constant up to 540 mL/min (corresponding to a residence time of $\tau_{res} = 27$ s).

4. Conclusions

In summary, a hyperpolarized ^{129}Xe gas generator incorporating a 210 W laser diode array has been described in which a nuclear polarization of 67% of ^{129}Xe has been attained. The ^{129}Xe nuclear polarization obtained with this LDA-based system is comparable to the best results achieved with a Ti:sapphire at low gas pressure and volume, but the capacity of the LDA system, in terms of the rate of ^{129}Xe magnetization produced, is far greater. The high polarization values, obtained with the UF-NHMFL polarizer, in comparison to previously described polarized gas generators, is attributed to (1) the high output power of our LDA system, (2) the relatively narrow laser line width of about 1.6 nm which allows lower buffer gas pressures to be employed, and (3) the use of pumping gas mixtures

with <1% Xe composition. We have systematically studied the effects of flow rate, laser power, pumping gas composition and temperature in order to maximize the xenon-129 nuclear polarization. It should be noted that working at smaller and smaller percentage composition of Xe gas will ultimately be limited by the practical difficulty of stripping sufficient quantities of polarized ^{129}Xe from the carrier gas. One would expect that in the cryogenic extraction process one must deal with the increasing heat load of the non-condensable He and N_2 gas on the condensed xenon.

The ability to generate quantities of highly polarized ^{129}Xe in excess of 1 L-atm/h will facilitate superior results in both 1D and 2D NMR experiments. Further improvements in performance are anticipated once temperature gradient and temperature control problems are remedied. The ability to utilize the 210 W laser system to achieve even higher P_z and MPF than reported here will depend on the ability to achieve more uniform excitation of the vapor and better temperature control of the pumping cell. One possibility being considered is to split the laser output into two parts in order to irradiate the pumping cell from both the front and rear by two counter-propagating beams of opposite helicity of the circular polarization. Optimization of the pumping cell and laser beam geometry may also mitigate the problems associated with temperature gradients at high laser power.

Potential spectroscopic applications that will directly benefit from increased polarization and capacity of ^{129}Xe gas include protein studies, surface NMR, and polarization transfer enhancement on surfaces and in solution.

Acknowledgments

The authors gratefully acknowledge receiving advice and assistance from Stephen Blackband, Samuel Grant, and Peter Thelwall. Anthony Zook was supported as a graduate research assistant by NIH Resource Grant P41 RR16105 (S. Blackband, PI). Funding for this project was also provided by the NHMFL In-House Research Program, the University of Florida and the NSF Major Research Instrumentation Grant CHE-9724635. The NHMFL is supported by NSF Cooperative Agreement No. DMR-9527035 and by the State of Florida. We wish to explicitly thank Jack Crow and Neil Sullivan for their support.

References

[1] D. Raftery, H. Long, T. Meersman, P.J. Grandinetti, L. Reven, A. Pines, Phys. Rev. Lett. 66 (1991) 584.
[2] B.M. Goodson, J. Magn. Res. 155 (2002) 157, and references therein.
[3] M.A. Bouchiat, T.R. Carver, C.M. Varnum, Phys. Rev. Lett. 5 (1960) 373.
[4] W. Happer, Rev. Mod. Phys. 44 (1972) 169.
[5] M.S. Albert et al., Nature (London) 370 (1994) 199.
[6] J.R. MacFall et al., Radiology 200 (1996) 553.
[7] Magnetic Imaging Technologies, Inc., Company Literature, 2500 Meridian Parkway, Suite 175, Durahm, NC 27713.
[8] B. Driehuys, G. Cates, E. Miron, K. Sauer, K. Walter, W. Happer, Appl. Phys. Lett. 69 (1996) 1668.
[9] U. Ruth, T. Hof, J. Schmidt, D. Fick, H.J. Jansch, Appl. Phys. B. 68 (1999) 93.
[10] C.H. Tseng, R.W. Mair, G.P. Wong, D. Williamson, D.G. Cory, R.L. Walsworth, Phys. Rev. E 59 (2001) 1785.
[11] R.G. Fitzgerald, K.L. Sauer, W. Happer, Chem. Phys. Lett. 284 (1998) 87.
[12] M. Haake, B.M. Goodson, D.D. Laws, E. Brunner, M.C. Cryier, R.H. Havlin, A. Pines, Chem. Phys. Lett. 292 (1998) 686.
[13] J.C. Leawoods, B.T. Saam, M.S. Conradi, Chem. Phys. Lett. 327 (2000) 359.
[14] R. Seydoux, A. Pines, M. Haake, J.A. Reimer, J. Phys. Chem. B 103 (1999) 4629.
[15] N. Shah, U. Timur, H. Wegener, H. Halling, K. Zilles, S. Appelt, NMR Biomed. 13 (2000) 214.
[16] R.C. Welsh, T.E. Chupp, K.P. Coulter, M.S. Rosen, S.D. Swanson, B.W. Agranoff, Nucl. Instr. Meth. A. 402 (1998) 461.
[17] J. Leawoods, B. Saam, M. Conradi, Chem. Phys. Lett. 327 (2000) 359.
[18] K. Ruppert, J.R. Brookman, K.D. Hagspiel, B. Driehuys, J.P. Mugler III, NMR Biomed. 13 (2000) 220.
[19] X.J. Chen et al., Magn. Res. Med. 42 (1999) 721.
[20] J. Kneller, R. Soto, S. Surber, J. Colomer, A. Fonseca, J. Nagy, T. Pietraß, J. Magn. Reson. 147 (2000) 261.
[21] T. Meersmann, J. Logan, R. Simonutti, S. Caldarelli, A. Comotti, P. Sozzani, L. Kaiser, A. Pines, J. Phys. Chem. A 104 (2000) 11665.
[22] L. Smith, J. Smith, E. MacNamara, K. Knagge, D. Raftery, J. Phys. Chem. B 105 (2001) 1412.
[23] L. Moudrakovski, S. Lang, C. Ratcliffe, B. Simard, G. Santyr, J. Ripmeester, J. Magn. Res 144 (2000) 372.
[24] G. Duhamel, unpublished results.
[25] It should be noted that Ruppert and Segebarth obtained these MPF values using flow rates corresponding to ^{129}Xe production rates in excess of 1 L-atm/h.
[26] National High Magnetic Field Laboratory, 1800 E. Paul Dirac Drive, Tallahassee, FL 32310.
[27] As measured by inversion recovery.
[28] Walter, W. Happer, Phys. Rev. Lett. 86 (2001) 3264.
[29] N.D. Bhaskar, W. Happer, T. McClelland, Phys. Rev. Lett. 49 (1982) 25.